PHOTONICS Research

Effective suppression of the photodarkening effect in high-power Yb-doped fiber amplifiers by H_2 loading

Ruiting Cao, Gui Chen,* Yisha Chen, Zhilun Zhang, Xianfeng Lin, Bin Dai, Luyun Yang, and Jinyan Li

Wuhan National Laboratory for Optoelectronics (WNLO), Huazhong University of Science and Technology, Wuhan 430074, China
**Corresponding author: chen_gui@hust.edu.cn*

Received 30 October 2019; revised 9 December 2019; accepted 16 December 2019; posted 18 December 2019 (Doc. ID 381208); published 13 February 2020

The radical suppression of the photodarkening effect and laser performance deterioration via H_2 loading were demonstrated in high-power Yb-doped fiber (YDF) amplifiers. The photodarkening loss at equilibrium was 114.4 dB/m at 702 nm in the pristine fiber, while it vanished in the H_2-loaded fiber. To obtain a deeper understanding of the impact of photodarkening on laser properties, the evolution of the mode instability threshold and output power in fiber amplifiers was investigated. After pumping for 300 min, the mode instability threshold of the pristine fiber dropped from 770 to 612 W, and the periodic fluctuation of the output power became intense, finally reaching 100 W. To address the detrimental effects originating from photodarkening, H_2 loading was applied in contrast experiments. The output power remained stable, and no sign of mode instability was observed in the H_2-loaded fiber. Moreover, the transmittance at 638 nm confirmed the absence of the photodarkening effect. The results pave the way for the further development of high-power fiber lasers.

https://doi.org/10.1364/PRJ.381208

1. INTRODUCTION

Fiber lasers have developed rapidly in the past few decades, breaking through 10 billion in the global market and surpassing other solid-state lasers to become the most dominant lasers. Yb-doped fibers (YDFs) are widely used in high-power applications owing to their low quantum loss, high conversion efficiency, and simple energy levels [1–3]. Up to now, the output power of single-mode YDF lasers has exceeded 20 kW [4].

However, YDFs are susceptible to the photodarkening (PD) effect, which reduces the long-term stability of fiber lasers [5]. PD will create color centers that can cause broad band absorption from the ultraviolet to the near infrared, inducing significant laser power decrease [6]. Since the absorption range of color centers covers the absorption and emission band of YDFs, it could absorb both pump light and signal light, producing a large amount of thermal load [7].

PD-induced thermal load can cause a series of issues. It could change the refractive index of the optical fiber via the thermo-optic effect, affecting the waveguide structure and thereby altering the bending loss of different modes [8]. More seriously, the thermal load induced by PD could distort the phase of the beam and aggravate thermally induced refractive index grating, which could eventually trigger the occurrence of mode instability (MI) [9,10]. As is known, MI depends on the phase shift between the thermally induced refractive index grating and the interference patterns formed by the fundamental mode (FM) and the high-order modes (HOMs) [11]. Otto *et al.* discovered the severe impact of PD on MI, and they considered PD as the second heat source in YDFs [10]. Even weak power loss induced by PD would significantly enhance the thermal load of optical fibers and sharply decline the MI threshold. Moreover, Ward *et al.* predicted that PD would give rise to quasi-static mode degradation on the scale of minutes or even hours [12]. They proposed that the unidirectional energy transfer from FM to HOM was caused by a phase-shifted refractive index grating. Afterwards, the mode degradation was experimentally observed in a pulse YDF amplifier, and the beam profile restored to Gaussian shape after 532 nm photobleaching, strongly supporting the theory of quasi-static mode degradation [13].

The mechanism of PD has not been determined yet; however, researchers have made great efforts to suppress PD. In terms of fiber fabrication, optimizing the doping composition by co-doping with Ce, P, Al, and Na ions into the fiber could inhibit PD to a certain extent [14–16]. It has been demonstrated that Yb/Ce fiber and Yb/Al/P fiber are applicable to suppress PD in high-power fiber lasers [17,18]. Also, reasonable design of the optical fiber structure could be conducive to

reducing mode overlap and thereby mitigating PD in laser operation [19]. Photobleaching and thermal bleaching were proposed to bleach the existing PD loss as well [6,20,21]. Moreover, the PD effect could also be suppressed by gas treatment including H_2 and O_2 [22–24]. Jasapara *et al.* placed the YDFs in a hydrogen environment and heated them for 14 h, and they found that the absorption spectrum remained unchanged under 976 nm pump [22]. Engholm *et al.* treated the YDFs with hydrogen at room temperature, and they found that the PD loss at 600 nm was strongly suppressed under 915 nm pump power [24]. Besides inhibiting PD, it was reported that H_2-loaded fiber exhibits excellent thermal performance in fiber lasers [25]. However, there is a lack of experimental investigation on the performance of H_2-loaded fiber in high-power applications. The influence of H_2 on output power degradation and MI threshold variation in a high-power system cannot be determined only by the absorption spectrum. In view of the excellent performance of H_2-loaded fiber, the effects of H_2 loading in high-power fiber amplifiers were examined.

In this work, the effective suppression of the PD effect and laser performance degradation through the H_2-loading technique in high-power fiber amplifiers were demonstrated. PD characteristics were explored both in the pristine fiber and the H_2-loaded fiber. The H_2-loaded fiber exhibited excellent PD resistance. For revealing the impact of PD on the laser properties in fiber amplifiers, long-term stability tests were performed. In the pristine fiber, the MI threshold was initially 770 W, decreasing by more than 20% after operating for 300 min, and the output power fluctuation increased to 100 W. Moreover, the transmittance at 638 nm revealed the nonuniform distribution of excess loss by the PD effect along the fiber. The H_2-loading technique was applied to mitigate PD, and it showed superior performance in stabilizing the output power and MI threshold. Transmittance of 638 nm was measured, and no sign of the PD effect was observed. Based on the results, the mechanism of H_2 loading in suppressing PD and stabilizing the fiber amplifier was discussed.

2. EXPERIMENTAL SETUP

In this experiment, a Yb/Al preform was fabricated by the modified chemical vapor deposition (MCVD) process combined with a solution doping method. The doping concentrations of the Yb and Al ions were 0.94% and 0.53% (mass fractions), respectively. The numerical aperture of the preform was 0.0596, with refractive index of the core and cladding of 1.451225 and 1.45, respectively. Based on the experimental condition, the PD loss measurement system could only be used for characterizing the performance of 10/130 μm fiber. However, 10/130 μm fiber was not suitable for high-power application at kilowatts. The output power was limited by the nonlinear effect due to the small mode field diameter. Thus, the preform was drawn into a 10/130 μm (N1) double-clad fiber for PD performance characterization and a 20/400 μm (N2) double-clad fiber for high-power application. The fiber was treated with 100% H_2 under 4 atm pressure for two weeks.

The measurement scheme of the PD-induced excess loss is shown in Fig. 1(a), and it adopted the same methodology as in previous research [14]. The laser properties were explored in a high-power master oscillator power amplifier (MOPA) system, which is depicted in Fig. 1(b). The experiment setup consisted of a seed source and a high-power amplification stage. The seed source was driven by a fiber oscillator emitting at 1080 nm, where six 915 nm laser diodes (LDs) were coupled to the combiner and injected into a 20/400 YDF. A pair of fiber Bragg gratings (FBGs) providing 99% and 10% reflectivity at 1080 nm comprised the resonant cavity. After filtering by a cladding light stripper (CLS), the output power of the seed was 45 W. At the amplification stage, six 976 nm LDs were coupled into the fiber under test via a combiner, which provided 1138 W pump power in total. The bending diameter of the fiber under test was 15 cm. Another CLS was applied to remove the cladding light, and an endcap was used to reduce the backlight. Moreover, the photodetector was placed on the CLS in the amplifier stage to detect the leaking light of the CLS and monitor the emergence of MI. The photodetector was connected with an oscilloscope to record the time trace of the leaking power from the CLS, and the standard deviation (STD) was obtained from the time trace for characterizing the emergence of MI.

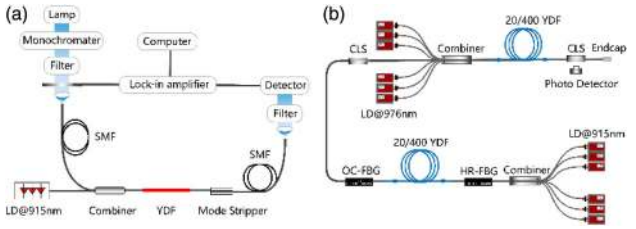

Fig. 1. (a) Measurement scheme of PD loss; (b) structure of high-power MOPA system.

The PD effect in the 20/400 YDFs was characterized by measuring the transmittance at 638 nm. A 638 nm single-mode LD provided maximum output power of 40 mW, serving as the probe. The pigtail of the 638 nm LD was 10/130 μm, which was connected to the homemade mode field adaptor. Then it was coupled to the 20/400 μm fiber under test, and the output power was measured by a power meter. The cutback method was used in the transmittance measurement of 638 nm.

3. EXPERIMENTAL RESULTS

A. Effect of H_2 Loading on PD Performance

First, the effect of H_2 loading on the PD properties in N1 fiber was investigated. The fiber under test was about 10 cm, and 915 nm LD was utilized as the pump source, with output power fixed at 5.5 W to provide an inversion level of about 45%. The absorption coefficient at 915 nm in N1 fiber was 0.90 dB/m, and the absorbed pump power was measured to be 0.2 W. The absorption spectra were measured every 20 min during the 300 min pumping process. Based on our previous research, the PD-induced excess losses at 633, 702, 810, and 1041 nm are selected to characterize the PD performance, and stretched exponential function fitting was used [26]. There is a linear relationship between PD loss at the selected wavelength and the laser operating wavelength at 1 μm [27]. The excess loss at 633 nm was commonly used in the characterization of PD

performance [28]; however, 633 nm was at the edge of the detection range of our measurement system, and the data fluctuates greatly. The PD-induced excess loss at 702 nm was 34.5 times that at 1041 nm, while the PD-induced excess loss at 810 nm was 9.5 times that at 1041 nm [27]. For accuracy, 702 nm was chosen for comparison in this work.

The absorption spectra before and after 300 min pumping of the pristine N1 fiber and the H_2-loaded N1 fiber are depicted in Fig. 2. Significant PD-induced absorption was observed in the pristine fiber during pumping, while it almost vanished in the range from 600 to 1100 nm in the H_2-loaded fiber. The time-dependent PD-induced excess losses of the pristine N1 fiber and the H_2-loaded N1 fiber are illustrated in Figs. 3(a) and 3(b). In the first hour, the PD loss at 702 nm of the pristine fiber rapidly increased to 34 dB/m, and it finally reached 64 dB/m at the end of pumping. The PD-induced excess loss did not reach equilibrium after 300 min pumping in the pristine fiber. The stretched exponential function is commonly used in PD performance description. Thus, the stretched exponential function fitting was applied in the experiment. By stretched exponential function fitting, the PD-induced equilibrium excess losses of the pristine fibers at 633, 702, 810, and 1041 nm were calculated to be 397.1, 114.4, 46.8, and 2.99 dB/m, respectively. For the H_2-loaded fiber, the PD-induced excess loss at 702 nm was less than 1 dB/m during the whole pumping process. In conclusion, the H_2-loaded fiber presented superior PD resistance when pumped with 915 nm.

B. Laser Performance of the Pristine Fiber

To further quantify the effect of PD on the laser properties in high-power fiber amplifiers, the evolution of the MI threshold and output power in the pristine N2 fiber were investigated during MOPA laser operation. The absorption coefficient of the N2 fiber at 976 nm is 1.05 dB/m. According to the research [29], the optimized length of N2 fiber was chosen to be 19 m in high-power fiber amplifiers. The total operating time of the system was 300 min. The MI threshold decreased with time, resulting in the instability of the system. To ensure the safety of system operation, the pump power was slightly reduced during operation. According to the pump power, the experiment was successively divided into three stages. Stage 1 occurred from 0 to 90 min, and the pump power was maintained at 822 W. Stage 2 occurred from 90 to 210 min, where the pump power was kept at 807 W. Stage 3 occurred from 210 to 300 min with pump power at 792 W.

The output power under 822 W pump power in stage 1 is shown in Fig. 4. The output power fluctuated, and the extent was increasing. In the first 20 min, the output power was relatively stable with fluctuation range of 20 W, which was caused by water-cooling system operation. Afterwards, the output power started to fluctuate quasi-periodically, with a period of about 3 min. The fluctuation amplitude increased with time and finally exceeded 100 W. The results implied the existence of PD-induced laser leakage, which could be confirmed by the temperature of the CLS. The variation trend of temperature in the CLS was opposite of the output power. When the output power decreased, the temperature increased sharply, indicating the huge increment of cladding power filtered by the CLS. Therefore, the pump power was reduced in the subsequent operation.

When the laser operated for 0, 30, 90, 150, 210, and 300 min, the MI thresholds were measured, and the output power as well as the STD is plotted in Fig. 5. For clarity, the STD data was marked with the dash line at 0.02, and the turning point before the power rollover phenomenon occurred was marked in red. At the beginning, the output power increased linearly with pump power, reaching a maximum output power at 770 W under pump power of 970 W, corresponding to an optical-optical efficiency of 79.4%. Further increasing the pump power, the power rollover phenomenon appeared, and the output power decreased rapidly along with the sharp STD increase. This indicated that the MI emerged at this moment, and the output power of the turning point was defined as the MI threshold, which was 770 W. To further confirm the occurrence of the MI phenomenon, the time-domain signal and the frequency-domain signal under pump power of

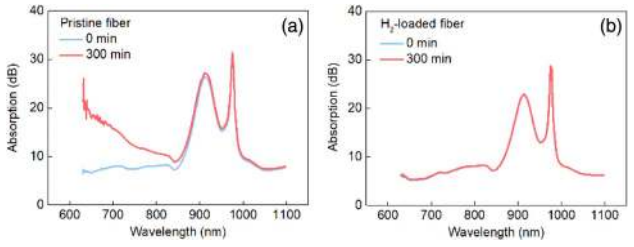

Fig. 2. Absorption spectra before and after 300 min pumping of (a) the pristine N1 fiber and (b) the H_2-loaded N1 fiber.

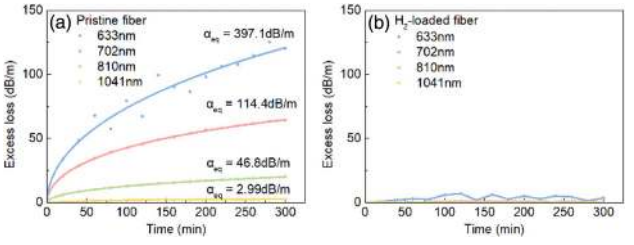

Fig. 3. PD-induced excess loss and fitting curve at 633, 702, 810, and 1041 nm for (a) the pristine N1 fiber and (b) the H_2-loaded N1 fiber.

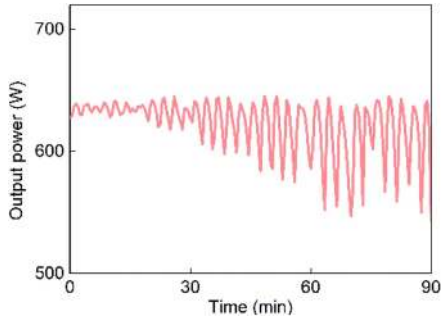

Fig. 4. Time dependence of the output power of the pristine N2 fiber.

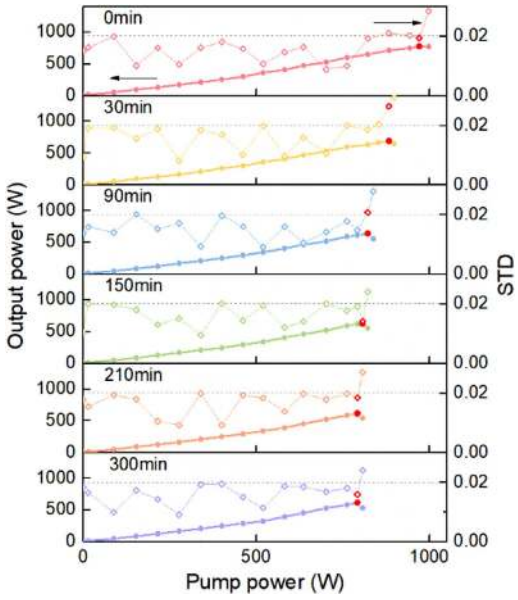

Fig. 5. Output power and STD as functions of pump power for the pristine N2 fiber.

998 W and 970 W, respectively, are shown in Fig. 6. The pumping power of 970 W corresponded to the turning point at 0 min. Under 970 W pumping, the time trace was stable, without a higher frequency component in the frequency spectra. When increasing the pump power to 998 W, the time trace exhibited intense fluctuation and a higher frequency component appeared. The result confirmed the existence of the MI phenomenon.

When the laser operated stably without the MI phenomenon, the fluctuations were relatively mild in the time trace and it exhibited random fluctuation in the STD, with no higher frequency component in the frequency domain. The output power raised steadily with the pump power increase, without sharp increase of the temperature in the CLS. When the MI phenomenon occurred, the fluctuation of the time trace became intense, showing a sharp increase in the STD, and higher frequency components were observed. A notable phenomenon of power rollover also appeared, manifesting as a sudden descent in the output power. Moreover, the filtered light raised rapidly in the CLS, accompanied with the intense temperature increase. The MI threshold was defined as the output power of the turning point before the power rollover phenomenon appeared.

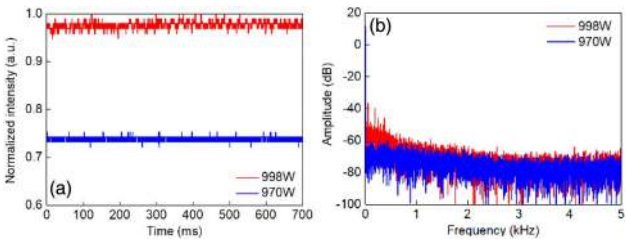

Fig. 6. Time-domain signal and frequency-domain signal of the pristine N2 fiber at the initial state.

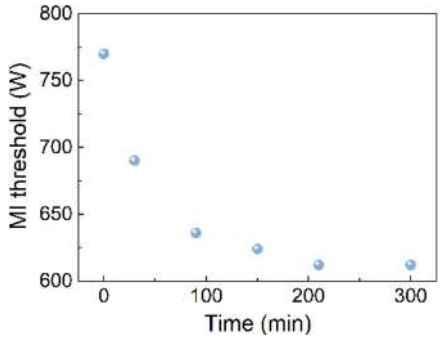

Fig. 7. Evolution of the MI threshold of the pristine N2 fiber.

After running for 30 min, the power rollover phenomenon took place in advance, when the output power exceeded 690 W, and the STD also increased significantly as shown in Fig. 5, which suggested that the MI threshold was 690 W. Compared with the MI threshold at 0 min, it decreased by more than 10% after running for 30 min. A similar phenomenon was observed in the subsequent tests, and the evolution of the MI threshold is plotted in Fig. 7. The MI threshold showed a downward trend in general, but the downward range was narrowed with laser operation duration. It decreased to 636, 624, and 612 W after operating for 90, 150, and 210 min, respectively. At the end of the operation, the MI threshold maintained at 612 W, reducing by more than 20% in contrast with the initial state.

Moreover, the 638 nm transmittances of the photodarkened N2 fiber were measured and compared with those of the pristine N2 fiber. First, the output power of the 19 m fiber was measured under 40 mW 638 nm light injection. Then, the input end was kept unchanged and the fiber was cut off from the output end to measure the output power at a different position. Finally, to avoid the influence of splicing loss, the output power of 638 nm light injected in 1 cm YDF was measured as the injection power. The results are depicted in Fig. 8. The transmittance of the pristine fiber stayed above 95%; by contrast, it presented a rapid declining trend in the photodarkened N2 fiber. The distribution of excess loss induced by the PD effect along the fiber was extremely nonuniform, with transmittance dropping by more than 70% in the front section and tending to

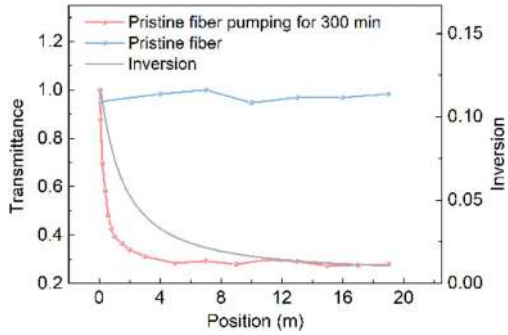

Fig. 8. Relative transmittance at 638 nm of the pristine N2 fiber before and after 300 min pumping, and the calculated inversion along the fiber.

be stable afterwards. Since the PD effect was closely related to the population inversion, it could be explained by the inversion. As shown in Fig. 8, the inversion was calculated according to the steady-state rate equations [30]. The inversion showed a similar variation tendency to the transmittance. In the co-pumped configurations, the fiber absorbed abundant pump power in the front section, while the signal light was weak, leading to undepleted inversion in the front section. Therefore, it created unevenly distributed PD loss along the fiber.

C. Laser Performance in the H_2-Loaded Fiber

In order to improve the PD resistance of the YDF and mitigate the impact of PD on a high-power MOPA system, the effects of H_2 loading on the laser properties of N2 fiber were explored. The length of the H_2-loaded fiber was 19 m to keep it consistent with the pristine fiber. To compare with the pristine fiber, the MOPA system operated under 822 W pump power for 300 min, and the output power was monitored.

The output power of the H_2-loaded fiber under 822 W pump is depicted in Fig. 9, and the output power of the pristine fiber is also shown for comparison. The intense fluctuation of output power with pumping time disappeared in the H_2-loaded fiber. In contrast with the pristine fiber, the output power of the H_2-loaded fiber showed excellent stability, with a fluctuation range of 20 W, which was within the experimental errors range. The slight differences between the output power might come from the differences in the efficiency of the two fibers.

The laser performance of the H_2-loaded fiber was explored when the laser operated for 0, 30, 90, 150, 210, and 300 min; besides, the STD was recorded. The results are illustrated in Fig. 10. At the beginning, when the pump power reached the maximum power at 1138 W, the output power was 932 W, corresponding to an optical-optical efficiency of 81.9%. In addition, there was no power rollover phenomenon, and the STD showed no significant increase. Based on the above results, there was no sign of MI occurrence. To verify the absence of the MI phenomenon, the time-domain signal and the frequency-domain signal under pump power of 1138 W and 1054 W, respectively, are shown in Fig. 11. In the time domain, the signal remained stable when pump power increased from 1054 to 1138 W. In the frequency domain, the higher frequency component was still absent, which confirmed that MI did not occur.

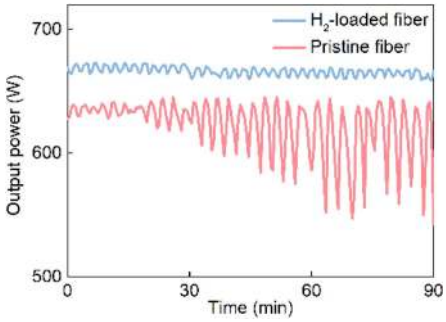

Fig. 9. Time dependence of output power in the H_2-loaded N2 fiber and the pristine fiber.

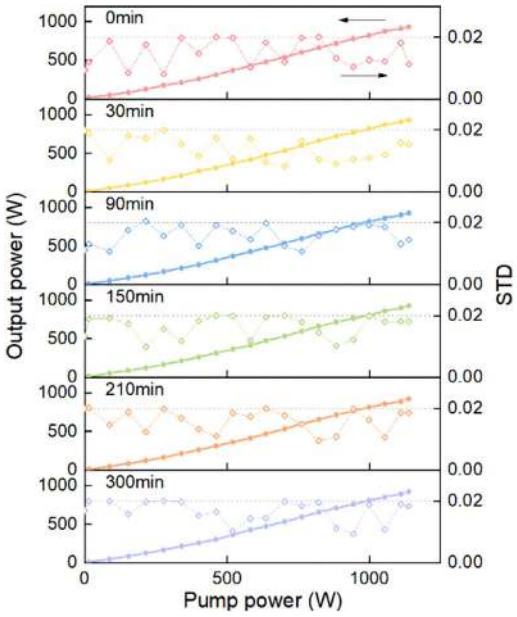

Fig. 10. Output power and STD as functions of pump power for the H_2-loaded N2 fiber.

When the laser operated for 30 min, the output power was 928 W under 1138 W pump power, which was basically consistent with the initial state, as shown in Fig. 10. No power rollover phenomenon was observed, and according to the STD, MI did not appear either. In the subsequent measurements of 90, 150, 210, and 300 min, the laser was stable with no sign of MI appearance. In the H_2-loaded fiber, the maximum output power was only limited by the pump power. The maximum output power slightly varied from 932 W at 0 min to 922 W at 300 min. Compared with the 20% decrease of the pristine fiber, the maximum output power fluctuated by 1% in the H_2-loaded fiber. The H_2-loaded fiber exhibited excellent performance of PD resistance and stabilizing the output power of high-power MOPA system in long-time operation.

To confirm the inhibitory effect on PD by H_2 loading, the transmittance at 638 nm was measured in the H_2-loaded N2 fiber after pumping for 300 min as shown in Fig. 12. The transmittance at 638 nm of the H_2-loaded fiber after operating for 300 min was basically consistent with that of the pristine fiber, demonstrating that the PD phenomenon was nearly nonexistent in the H_2-loaded fiber after 976 nm pumping.

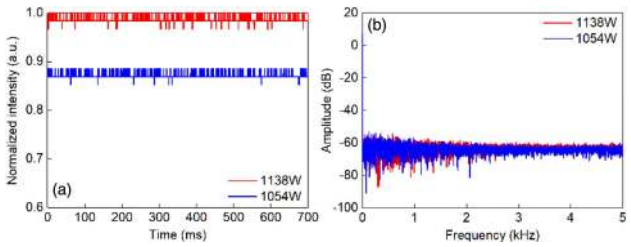

Fig. 11. Time-domain signal and frequency-domain signal of the H_2-loaded N2 fiber at the initial state.

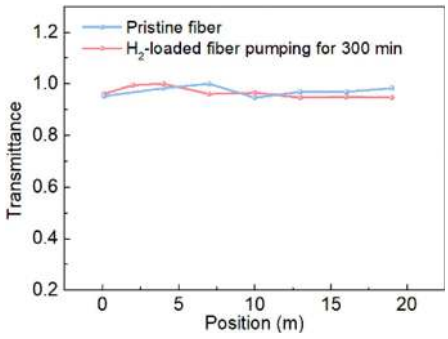

Fig. 12. Relative transmittance at 638 nm of the pristine N2 fiber and the H_2-loaded N2 fiber after 300 min pumping.

4. DISCUSSION

PD effect could be suppressed efficaciously through H_2 loading, and the inhibition mechanism is of great significance for revealing the origin of the PD effect and eliminating PD in turn. In Yb-doped aluminosilicate fibers, the nonbridging oxygen hole centers (NBOHCs) and the aluminum oxygen hole centers (AlOHCs) were considered to be important defects for causing PD [31,32]. Although the matrix in silica glass is dense in the structure, H_2 molecules are free to move in silica fiber. They can react with the dangling bonds of NBOHC to form a more stable covalent bond of -OH and to release electrons that could be bound with the hole-related defects and thus eliminate the related defects [33,34]. The schematic representation of H_2 cracking defects is shown in Fig. 13. This reaction is an exothermic reaction with 0.4 eV of energy being released. Furthermore, the energy barrier of H-H dissociation is 0.1 eV, implying that H_2 cracking NBOHC could occur even at low temperatures. They also predicted that H_2 molecules could react with other paramagnetic centers at room temperature. Hence, it could be inferred that a similar reaction may happen between H_2 molecules and AlOHCs, generating -OH bonds and erasing the defects, inhibiting the emergence of PD. Therefore, the H_2-loaded fiber exhibited excellent PD resistance.

In high-power applications, H_2-loaded fiber also exhibits superior performance in stabilizing the system and suppressing MI threshold degradation. It is widely accepted that the main cause of MI is thermal refractive index grating in optical fibers

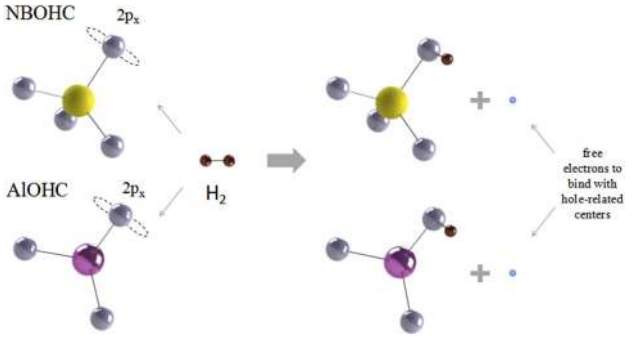

Fig. 13. Schematic representation of H_2 cracking NBOHC and AlOHC.

[11]. When MI arises, energy transfer occurs between FM and HOM. The precondition for the energy transfer is the phase shift between the interference pattern and the thermally induced refractive index grating. In our previous work, it was suggested that PD may exceed quantum defect (QD) to become the most dominant heat source [25]. The experimental results revealed that PD had a severe impact on MI threshold, which was in accordance with the report that PD loss would cause significant thermal load and lead to rapid falling of the MI threshold [10]. In the fiber amplifier, the undepleted inversion during laser operation would result in the generation of PD and the formation of color centers in the YDF, which could absorb the energy of both pumped light and signal light. It would result in thermal load accumulating in the optical fiber [25]. More importantly, the strength of the thermally induced refractive index grating could be enhanced. As a result, the MI threshold decreased with the strengthening of the PD effect. Furthermore, since a weak PD effect can cause a strong thermal load and affect the MI threshold seriously, reducing PD is an effective way to improve the MI threshold. Thus, the degradation of the MI threshold can be obviated by H_2 loading.

In the continuous operation, the MOPA system worked below the MI threshold, and the output power of the pristine fiber fluctuated periodically, while it disappeared in the H_2-loaded fiber. First, the PD-induced laser leakage phenomenon indicated the existence of energy transfer between the FM and HOM. It is mentioned that the strength of the thermally induced refractive index grating is sufficient for energy coupling at output power far below the MI threshold as long as the phase shift is large enough; in addition, the thermally induced refractive index grating is more sensitive to phase shift in high-power conditions [35]. Not considering the thermal load caused by PD, the phase shift would not exist below the MI threshold. The mode interference pattern and the thermally induced refractive index changes show left-right symmetry, and thus the strength of the mode coupling is zero [11]. However, the PD effect was strengthened continuously during the pumping process, leading to the gradual increase of thermal load and the continuous change in phase shift, which would break the left-right symmetry and allow mode coupling to occur. Moreover, according to the research [35], when a negative phase shift existed, the energy transferred from the FM to HOM, and a positive phase shift generated energy transfer from the HOM to FM. Thus, the periodic energy transfer between the FM and HOM was sustainable, even if the system operated far below the MI threshold. Second, the nonuniform distribution of excess loss induced by the PD effect varied the bending loss of different modes via thermal effect [8]. The PD effect was more serious in the front section of the fiber, generating severe thermal load. The heat increased the refractive index and decreased the bending loss of the HOM, confining the HOM in the core. However, when light propagated to the later part of the fiber, the PD effect was relieved, and the resulting thermal load went down. In consequence, the bending loss of the HOM increased, and the HOM was coupled from the core into the cladding. Due to the filtration effect of CLS, the HOM in the cladding was filtered out, manifesting as the decline of the output power. Third, an output

power oscillation period of about 3 min was observed in this work. Kong *et al.* also reported the output power fluctuation with operating time in fiber amplifiers, and the output power perturbation period was about 4–6 min [36]. The result in this work was similar to their observation. However, the YDF and the laser operating parameters such as the seed power, the pump wavelength, and the pump power were different in these two works, which caused the discrepancy in the oscillation period. The period could be influenced by the PD rate. When the PD rate is increased, the thermal load induced by PD is raised. This would enhance the rate of change in the phase shift between mode interference and thermally induced refractive index grating; therefore, the period of power coupling would be reduced. Fourth, with the PD effect continuing to rise in the long term, the average strength of the thermally induced refractive index grating ascended, and the mode coupling from the FM to HOM became more intense. Compared with the initial state, the filtered HOM energy kept ascending, which led to the severe decline of output power. Since the PD-induced laser leakage originated from the thermal load induced by PD, the elimination of the PD effect via H_2 loading could efficaciously address the issue.

5. CONCLUSION

A detailed investigation of PD-induced laser property degradation and mitigation through H_2 loading in high-power YDF amplifiers was presented. PD-induced excess loss was completely suppressed by H_2 loading. For high-power application, the MI threshold of the pristine fiber declined by 20% after operating for 300 min. Simultaneously, the output power presented periodic fluctuations with the amplitude exceeding 100 W. H_2 loading can effectively improve the long-term stability of high-power fiber amplifiers. In the H_2-loaded fiber, the output power remained stable during the whole pumping process, and MI did not occur. The suppressing effect on PD may be attributed to the reaction between H_2 molecules and defects such as AlOHC and NBOHC, forming a stable covalent bond of -OH. Thus, it is indicated that H_2-loading technology will play an important role in inhibiting PD and stabilizing the operation of high-power YDF lasers.

Funding. National Natural Science Foundation of China (61735007); National Key Research and Development Program of China (2017YFB1104400).

Disclosures. The authors declare no conflicts of interest.

REFERENCES

1. C. Jauregui, J. Limpert, and A. Tünnermann, "High-power fibre lasers," Nat. Photonics **7**, 861–867 (2013).
2. J. Nilsson and D. N. Payne, "Physics: high-power fiber lasers," Science **332**, 921–922 (2011).
3. D. J. Richardson, J. Nilsson, and W. A. Clarkson, "High power fiber lasers: current status and future perspectives," J. Opt. Soc. Am. B **27**, B63–B92 (2010).
4. B. Shiner, "The impact of fiber laser technology on the world wide material processing market," in *Conference on Lasers and Electro-Optics* (Optical Society of America, 2013), paper AF2J.1.
5. C. Ye, L. Petit, J. J. Koponen, I.-N. Hu, and A. Galvanauskas, "Short-term and long-term stability in ytterbium-doped high-power fiber lasers and amplifiers," IEEE J. Sel. Top. Quantum Electron. **20**, 0903512 (2014).
6. I. Manek-Hönninger, J. Boullet, T. Cardinal, F. Guillen, S. Ermeneux, M. Podgorski, R. B. Doua, and F. Salin, "Photodarkening and photobleaching of an ytterbium-doped silica double-clad LMA fiber," Opt. Express **15**, 1606–1611 (2007).
7. J. J. Montiel, I. Ponsoda, M. J. Söderlund, J. P. Koplow, J. J. Koponen, and S. Honkanen, "Photodarkening-induced increase of fiber temperature," Appl. Opt. **49**, 4139–4143 (2010).
8. L. Kong, J. Leng, P. Zhou, and Z. Jiang, "Thermally induced mode loss evolution in the coiled ytterbium doped large mode area fiber," Opt. Express **25**, 2639–2648 (2017).
9. Y. Feng, B. M. Zhang, and J. Nilsson, "Photodarkening-induced phase distortions and their effects in single-channel and coherently combined Yb-doped fiber chirped pulse amplification systems," J. Lightwave Technol. **36**, 5521–5527 (2018).
10. H. Otto, N. Modsching, C. Jauregui, J. Limpert, and A. Tünnermann, "Impact of photodarkening on the mode instability threshold," Opt. Express **23**, 15265–15277 (2015).
11. A. V. Smith and J. J. Smith, "Mode instability in high power fiber amplifiers," Opt. Express **19**, 10180–10192 (2011).
12. B. Ward, "Theory and modeling of photodarkening-induced quasi static degradation in fiber amplifiers," Opt. Express **24**, 3488–3501 (2016).
13. K. K. Bobkov, M. M. Bubnov, S. S. Aleshkina, and M. E. Likhachev, "Long-term mode shape degradation in large mode area Yb-doped pulsed fiber amplifiers," Laser Phys. Lett. **14**, 015102 (2017).
14. N. Zhao, Y. Liu, M. Li, J. Li, J. Peng, L. Yang, N. Dai, H. Li, and J. Li, "Mitigation of photodarkening effect in Yb-doped fiber through Na^+ ions doping," Opt. Express **25**, 18191–18196 (2017).
15. M. Engholm, P. Jelger, F. Laurell, and L. Norin, "Improved photodarkening resistivity in ytterbium-doped fiber lasers by cerium codoping," Opt. Lett. **34**, 1285–1287 (2009).
16. S. Jetschke, S. Unger, A. Schwuchow, M. Leich, and J. Kirchhof, "Efficient Yb laser fibers with low photodarkening by optimization of the core composition," Opt. Express **16**, 15540–15545 (2008).
17. S. Liu, K. Peng, H. Zhan, L. Ni, X. Wang, Y. Wang, Y. Li, J. Yu, L. Jiang, R. Zhu, J. Wang, F. Jing, and A. Lin, "3 kW 20/400 Yb-doped aluminophosphosilicate fiber with high stability," IEEE Photon. J. **10**, 1503408 (2018).
18. Y. Li, S. Liu, H. Zhan, K. Peng, S. Sun, J. Jiang, X. Wang, L. Ni, L. Jiang, J. Wang, F. Jing, and A. Lin, "Fiber design and fabrication of Yb/Ce codoped aluminosilicate laser fiber with high laser stability," IEEE Photon. J. **10**, 1502908 (2018).
19. K. E. Mattsson, "Low photo darkening single mode RMO fiber," Opt. Express **17**, 17855–17861 (2009).
20. M. Leich, U. Röpke, S. Jetschke, S. Unger, V. Reichel, and J. Kirchhof, "Non-isothermal bleaching of photodarkened Yb-doped fibers," Opt. Express **17**, 12588–12593 (2009).
21. R. Cao, X. Lin, Y. Chen, Y. Cheng, Y. Wang, Y. Xing, H. Li, L. Yang, G. Chen, and J. Li, "532 nm pump induced photo-darkening inhibition and photo-bleaching in high power Yb-doped fiber amplifiers," Opt. Express **27**, 26523–26531 (2019).
22. J. Jasapara, M. Andrejco, D. DiGiovanni, and R. Windeler, "Effect of heat and H_2 gas on the photo-darkening of Yb^{3+} fibers," in *Conference on Lasers and Electro-Optics* (Optical Society of America, 2006), paper CTuQ5.
23. S. Yoo, C. Basu, A. J. Boyland, C. Sones, J. Nilsson, J. K. Sahu, and D. Payne, "Photodarkening in Yb-doped aluminosilicate fibers induced by 488 nm irradiation," Opt. Lett. **32**, 1626–1628 (2007).
24. M. Engholm and L. Norin, "Reduction of photodarkening in Yb/Al-doped fiber lasers," Proc. SPIE **6873**, 68731E (2008).
25. R. Cao, Y. Wang, G. Chen, N. Zhao, Y. Xing, Y. Liu, X. Lin, Y. Cheng, H. Li, L. Yang, and J. Li, "Investigation of photo-darkening induced thermal load in Yb-doped fiber lasers," IEEE Photon. Technol. Lett. **31**, 809–812 (2019).
26. S. Jetschke and U. Röpke, "Power-law dependence of the photodarkening rate constant on the inversion in Yb doped fibers," Opt. Lett. **34**, 109–111 (2009).
27. G. Chen, L. Xie, Y. B. Wang, N. Zhao, H. Q. Li, Z. W. Jiang, J. G. Peng, L. Y. Yang, N. L. Dai, and J. Y. Li, "Photodarkening-induced

absorption and fluorescence changes in Yb fibers," Chin. Phys. Lett. **30**, 104208 (2013).
28. S. Jetschke, S. Unger, U. Röpke, and J. Kirchhof, "Photodarkening in Yb doped fibers: experimental evidence of equilibrium states depending on the pump power," Opt. Express **15**, 14838–14843 (2007).
29. J. W. Dawson, M. J. Messerly, R. J. Beach, M. Y. Shverdin, E. A. Stappaerts, A. K. Sridharan, P. H. Pax, J. E. Heebner, C. W. Siders, and C. P. J. Barty, "Analysis of the scalability of diffraction-limited fiber lasers and amplifiers to high average power," Opt. Express **16**, 13240–13266 (2008).
30. C. Jauregui, H.-J. Otto, F. Stutzki, J. Limpert, and A. Tünnermann, "Simplified modelling the mode instability threshold of high power fiber amplifiers in the presence of photodarkening," Opt. Express **23**, 20203–20218 (2015).
31. T. Deschamps, H. Vezin, C. Gonnet, and N. Ollier, "Evidence of AlOHC responsible for the radiation-induced darkening in Yb doped fiber," Opt. Express **21**, 8382–8392 (2013).
32. P. D. Dragic, C. G. Carlson, and A. Croteau, "Characterization of defect luminescence in Yb doped silica fibers: part I NBOHC," Opt. Express **16**, 4688–4697 (2008).
33. M. Vitiello, A. N. Lopez, F. Illas, G. Pacchioni, N. Lopez, F. Illas, G. Pacchioni, A. N. Lopez, F. Illas, G. Pacchioni, N. Lopez, F. Illas, and G. Pacchioni, "H_2 cracking at SiO_2 defect centers," J. Phys. Chem. A **104**, 4674–4684 (2000).
34. Y.-B. Xing, Y.-Z. Liu, N. Zhao, R.-T. Cao, Y.-B. Wang, Y. Yang, J.-G. Peng, H.-Q. Li, L.-Y. Yang, N.-L. Dai, and J.-Y. Li, "Radical passive bleaching of Tm-doped silica fiber with deuterium," Opt. Lett. **43**, 1075–1078 (2018).
35. C. Stihler, C. Jauregui, A. Tünnermann, and J. Limpert, "Modal energy transfer by thermally-induced refractive index gratings in Yb-doped fibers," Light Sci. Appl. **7**, 59 (2018).
36. L. Kong, M. Li, J. Leng, X. Wang, and P. Zhou, "Experimental investigation of the photodarkening induced core laser leakage in a 3 kW co-pumping fiber amplifier," Proc. SPIE **10436**, 104360N (2017).